Scientific Research Publishing

American Journal of Plant Sciences, 2022, 13, 943-959
https://www.scirp.org/journal/ajps
ISSN Online: 2158-2750
ISSN Print: 2158-2742

A Putative Protein with No Known Function in *Arabidopsis thaliana* Harbors a Domain with Adenylyl Cyclase Activity

Katlego S. Sehlabane, Patience Chatukuta, Tshegofatso B. Dikobe, Enetia D. Bobo, Angela Sibanda, David T. Kawadza, Oziniel Ruzvidzo*

Department of Botany, North-West University, Mmabatho, South Africa
Email: *Oziniel.Ruzvidzo@nwu.ac.za

How to cite this paper: Sehlabane, K.S., Chatukuta, P., Dikobe, T.B., Bobo, E.D., Sibanda, A., Kawadza, D.T. and Ruzvidzo, O. (2022) A Putative Protein with No Known Function in *Arabidopsis thaliana* Harbors a Domain with Adenylyl Cyclase Activity. *American Journal of Plant Sciences*, **13**, 943-959.
https://doi.org/10.4236/ajps.2022.137062

Received: May 7, 2022
Accepted: July 15, 2022
Published: July 18, 2022

Abstract

Adenylyl cyclases (ACs) are a special group of enzymes that catalyze formation of the second messenger molecule, 3',5'-cyclic adenosine monophosphate (cAMP) from 5'-adenosine triphosphate (ATP). Apparently, even though cAMP is increasingly becoming an important signaling molecule in higher plants, the identification of plant ACs has somewhat remained slow. Here we report the recombinant cloning, partial expression and affinity purification of the truncated version ($AtAC^{261-388}$) of a putative *Arabidopsis thaliana* protein (AtAC: At3g21465) followed by a demonstration of its inherent enzymatic activity as an AC. Currently, AtAC is not assigned any particular function in *A. thaliana* but simply annotated as an AC-like protein and, therefore, we targeted it for our study to establish if it is indeed a *bona fide* AC molecule. From our work, we firstly, show through enzyme immunoassaying and mass spectrometry that the recombinant $AtAC^{261-388}$ can generate cAMP from ATP *in vitro* in a manganese-dependent manner that is activated by calcium and hydrogen carbonate. Secondly, we reveal through computational analysis that the AC center of AtAC is solvent-exposed, and amenable to the unhindered access of ATP as a substrate for catalysis. Lastly, we show that the recombinant $AtAC^{261-388}$ can complement AC-deficiency (*cya*A mutation) in SP850 cells when expressed in this mutant *Escherichia coli* strain.

Keywords

Arabidopsis thaliana, Adenylyl Cyclase, Enzyme Immunoassay, Mass Spectrometry, Computational Analysis

1. Introduction

Adenylyl cylases (ACs) are enzymes capable of generating 3',5'-cyclic adenosine

monophosphate (cAMP) from 5'-adenosine triphosphate (ATP). By the mid-1970s, these two molecules (ACs and cAMP) had been firmly established as important signaling molecules in both the animal and lower eukaryotic systems [1] [2] [3], where they affect many different biochemical and physiological processes, including the activity of kinases [1]. Therefore, given the then growing realization of the significant importance of these two molecules in animals and lower eukaryotes, it is not surprising that plant scientists were keen to learn and understand if these same molecules and their associated signaling systems were universal and thus also similarly operating in plants.

Apparently, the major reasons why either the presence or functions of ACs and cAMP were more difficult to establish in plants than in other organisms were; firstly, that the levels of cAMP detected in plants appeared to be so low (<20 pmol/g fresh weight) [4] compared to those found in animals (>250 pmol/g wet weight) [5] and secondly, that the vagaries of assaying systems used by then in plants were not conducive to reach firm conclusions [6]. However, some specific pathogen-induced signaling at lower cyclic nucleotide (CN) concentrations had already been reported in plants [7], while a cell-permeant 8-Br-cAMP and the stimulation of *albeit* unknown ACs with forskolin had also been shown to elicit concentration- and time-dependent plant biological responses such as increases in Ca^{2+} influx across the plasma membrane [8]. In addition, some biochemical evidence had also suggested that crude alfalfa (*Medicago sativa* L.) root extracts could show a calmodulin-dependent AC activity [9]. Arguably, the most convincing data for a specific signaling role of cAMP came from whole-cell patch-clamp recordings from *Vicia faba* mesophyll protoplasts, which revealed that outward K^+ currents, could increase in a dose-dependent fashion as a result of the intracellular application of cAMP but not 5'-adenosine monophosphate (AMP), 3',5'-cyclic guanosine monophosphate (cGMP) or 5'-guanosine monophosphate (GMP) [10].

Following this and with time, many processes that are cAMP-dependent were then conclusively reported in plants. This was as a result of both the emergency and availability of advanced analytical tools that then dramatically improved the assaying systems in plants and ultimately, the inference of solid conclusions [6]. The reported processes include control of the cell cycle in tobacco [11], transport of sodium ions via the voltage-independent channels (VICs) in *Arabidopsis thaliana* [12], stomatal closure in *Vicia faba* [13], growth of pollen tubes in *Agapanthus umbellatus*, *Lilium longiflorum* and *Zea mays* [14] [15], activation of the phenylalanine ammonia lyase (PAL) enzyme in French beans [16] and regulation of the phenylpropanoid pathway in *A. thaliana* [17]. ACs and cAMP were also found to be involved in stress response [18] [19] [20] [21] primarily via the cyclic nucleotide-gated channels (CNGCs) [22].

Later on, the first-ever plant AC was then identified in maize using recombinant expression and complementation testing [15], followed by further identification of ten more ACs through motif-based searches [23]-[31] and phylogenetic studies [20] [21] [32]. Nevertheless, and considering the number and diverse

nature of processes currently known to be cAMP-dependent in plants, these identified ACs are still very few.

Therefore in an attempt to identify yet another plant AC and the potential advancement of ACs and cAMP in plants (including crops), we targeted an *A. thaliana* protein (AtAC) previously predicted to be an AC-like molecule (http://www.ncbi.nlm.nih.gov/protein/51968402) and demonstrated its capability to generate cAMP from ATP as a functional AC.

2. Materials and Methods

2.1. Generation of the AtAC$^{260\text{-}388}$ Recombinant Protein

Total RNA was extracted from six-week-old *Arabidopsis thaliana* ecotype Columbia-0 (Col-0) seedlings using the RNeasy plant mini kit, in combination with DNase 1 treatment, as instructed by the manufacturer (Qiagen, Crawley, UK). Copy DNA (cDNA) sequence of At3g21465 was retrieved from The Arabidopsis Information Resource (TAIR) (https://www.arabidopsis.org/) and verified for presence of the AC catalytic center using the PROSITE database located within the Expert Protein Analysis System (ExPASy) proteomics server (https://www.expasy.org/). At3g21465 cDNA synthesis from the total RNA and subsequent amplification of the AtAC$^{260\text{-}388}$ gene fragment from the cDNA were simultaneously performed in the presence of two sequence-specific primers (forward: 5'-GCTGCCAAAAGAGGAGACACAGAGTCGTTA-3' and reverse: 5'-GCTAAGAAGAGCTTCATTCTTGTTTAACTC-3' using a Verso 1-Step RT-PCR kit and in accordance with the manufacturer's instructions (Thermo Scientific, Rockford, USA). The PCR product was then cloned into a pTrcHis2-TOPO expression vector via the TA cloning system (Invitrogen Corp., Carlsbad, USA) to make a pTrcHis2-TOPO:AtAC$^{260\text{-}388}$ fusion expression construct with a C-terminus His purification tag. Expression, purification and refolding processes of the recombinant AtAC$^{260\text{-}388}$ protein were undertaken as outlined below and detailed elsewhere [26] [33]. The relative molecular mass of the generated AtAC$^{260\text{-}388}$ was estimated using the ProtParam tool on the ExPasy Proteomics Server (http://au.expasy.org/tool/.protpatram.html). Whereas the purified AtAC$^{260\text{-}388}$ protein was used for *in vitro* activity assays, the produced pTrcHis2-TOPO:AtAC$^{260\text{-}388}$ fusion expression construct was used for complementation testing.

2.1.1. Expression of AtAC$^{260\text{-}388}$

The generated pTrcHis2-TOPO:AtAC$^{260\text{-}388}$ fusion expression construct was used to transform (through heat shock at 42˚C for 2 min) chemically competent *E. coli* EXPRESS BL21 (DE3) pLysS DUOs cells (Lucigen Corp., Wisconsin, USA). The transformed cells were then grown in double strength yeast-tryptone (2YT) media (16 g/L tryptone, 10 g/L yeast extract, 5 g/L NaCl and 4 g/L glucose; pH 7.0) supplemented with 100 µg/ml ampicillin and 34 µg/ml chloramphenicol, on an orbital shaker (250 rpm) at 37˚C. To induce expression, 1 mM of isopropyl-β-D-thiogalactopyranoside (IPTG, Sigma-Aldrich Corp, Missouri) was

added to the media when the optical density (OD_{600}) of the cell culture had reached 0.5 (approximately 2 h). The culture was then left to grow for a further 3 h at 37˚C at 250 rpm.

2.1.2. Purification of AtAC$^{260\text{-}388}$

The expressed recombinant AtAC$^{260\text{-}388}$ protein was purified by preparing a cleared cell lysate of the induced *E. coli* EXPRESS BL21 (DE3) pLysS DUOs cells under non-native denaturing conditions, where the harvested cells were resuspended in a urea lysis buffer (8 M urea, 100 mM NaH_2PO_4, 10 mM Tris-HCl; pH 8.0, 500 mM NaCl, 20 mM β-mercaptoethanol, 10 mM imidazole and 7.5% (v/v) glycerol) at a ratio of 1 g pellet to every 10 ml buffer and mixing thoroughly with a magnetic stirrer for 1 h at 24˚C. The mixture was then centrifuged at 2500x*g* for 15 min and the supernatant collected as cleared lysate. The collected cleared lysate was transferred to 2 ml of 50% (w/v) nickel-nitriloacetic acid (Ni-NTA) slurry (Catalog # P6611; Sigma-Aldrich Corp., Missouri, USA) pre-equilibrated with 10 ml of lysis buffer and the two components gently mixed on a rotary mixer for 1 h at 24˚C. This step allowed for binding of the His-tagged AtAC$^{260\text{-}388}$ protein onto the Ni-NTA resin. The cleared lysate-resin mixture was then loaded into an empty XK16 column (Bio-Rad Laboratories Inc., California, USA), allowed to settle and the flow-through discarded. The protein-bound resin was then washed three times with 30 ml of wash buffer (8 M urea, 100 mM NaH_2PO_4, 10 mM Tris-Cl; pH 8.0, 500 mM NaCl, 20 mM β-mercaptoethanol, 7.5% (v/v) glycerol, and 40 mM imidazole) to remove unbound proteins.

2.1.3. Refolding of AtAC$^{260\text{-}388}$

The washed protein-bound resin was pre-equilibrated with 3 ml of refolding buffer A (8 M urea, 200 mM NaCl, 50 mM Tris-Cl; pH 8.0, 500 mM glucose, 0.05% (w/v) poly-ethyl glycol (PEG), 20 mM β-mercaptoethanol) in preparation for protein refolding on a Bio-Logic F40 Duo-Flow chromatography system (Bio-Rad Laboratories., California, USA). The denatured and purified recombinant AtAC$^{260\text{-}388}$ was then refolded into its native soluble form using a controlled linearized gradient system, whereby the 8 M urea salt in the refolding buffer A was gradually diluted to 0 M concentration using a refolding buffer B (200 mM NaCl, 50 mM Tris-Cl; pH 8.0, 500 mM glucose, 0.05% (w/v) poly-ethyl glycol (PEG), 4 mM reduced glutathione, 0.4 mM oxidized glutathione, and 0.5 mM phenylmethanesulfonylfluoride (PMSF)). The refolding process of the denatured AtAC$^{260\text{-}388}$ was run for 13 h at a flow-rate of 0.5 ml/min. After refolding, the renatured recombinant AtAC$^{260\text{-}388}$ was then eluted off the Ni-NTA resin in 2 ml of the non-denaturing native elution buffer (200 mM NaCl, 50 mM Tris-Cl; pH 8.0, 250 mM imidazole, 20% (v/v) glycerol, and 0.5 mM PMSF). The eluted native protein fraction was then freed from its buffering salts and excess water using a Spin-X UF concentrator device with a molecular weight cut off (MWCO) point of 5000 (Product # 431482; Corning Life Sciences Corp., New York, USA) and in accordance with the manufacturer's instructions. Concentration of the resulting

eluted AtAC$^{260\text{-}388}$ protein was then determined through the Bradford method [34] and spectrophotometrically using an ND2000 nanodrop (Thermo Scientific Inc., California, USA).

2.2. Determination of the *in Vitro* AC Activity of AtAC$^{260\text{-}388}$

The AC activity of the purified recombinant AtAC$^{260\text{-}388}$ was determined *in vitro* by incubating 5 µg of the protein in 50 mM Tris-Cl; pH 8.0, 2 mM isobutylmethylxanthine (IBMX, Sigma-Aldrich Corp., Missouri, USA) to inhibit phosphodiesterases, 5 mM Mg^{2+} or Mn^{2+} and 1 mM ATP with or without 250 µM Ca^{2+} or 50 mM HCO_3^-, in a final volume of 200 µl, followed by measurement of the generated cAMP. Levels of the generated cAMP were determined by enzyme immunoassaying following its acetylation protocol as described by the supplier's manual (Sigma-Aldrich Corp., Missouri, USA; code: CA201) and as is detailed elsewhere [25] [26]. Background cAMP levels in control reactions were measured in tubes that contained the incubation mediums but no protein or Ca^{2+} or HCO_3^-. In all cases, reactions were incubated at room temperature (24˚C) for 20 min and then terminated by adding 10 mM EDTA followed by boiling for 5 min and then cooling on ice for 2 min before centrifugation at 2300x*g* for 3 min. The resulting supernatant was then assayed for cAMP content through reading at 405 nm using a calorimetric microplate reader (Labtech International Limited, East Sussex, UK).

2.3. Detection of cAMP by Mass Spectrometry

The acetylated cAMP samples generated from the *in vitro* AC activity assays were introduced into a Waters API Q-TOF Ultima mass spectrometer (Waters Microsep, Johannesburg, RSA) with a Waters Acquity UPLC at a flow rate of 180 ml/min. Separation was achieved in a Phenomenex Synergi (Torrance, CA) 4 µm Fusion-RP (250 × 2.0 mm) column when a gradient of solvent "A" (0.1% formic acid) and solvent "B" (100% acetonitrile) was applied over 18 min. During the first 7 min, the solvent composition was kept at 100% "A" followed by a linear gradient of up to 80% "B" for 3 min, and then a re-equilibration to the initial conditions. An electrospray ionization in the negative (W-) mode was used at a cone voltage of 35 V, to detect molecules and generate chromatograms.

2.4. Computational Analysis of AtAC

A 3-dimensional (3D) model of AtAC was constructed by artificial intelligence using AlphaFOLD [35]. This software uses a neural network-based model of artificial intelligence to predict protein structures from their amino acid sequences with an atomic accuracy level. It first aligns the amino acid sequence input with sequences of known structures for pair-wise representation. The representation is then used to produce atomic coordinates for each residue, thus predicting the necessary rotation and then assembling a structured chain of amino acid residues. Its developers freely provide the source code for access to trained modelers

and a script for predicting structures of novel input sequences [35]. In our case, the full-length amino acid sequence of AtAC was submitted to the AlphaFOLD database followed by downloading of the model with the highest quality (based on C-scores). The downloaded model was visualized and analyzed using UCSF ChimeraX (v.1.10.1.) [36]. SeeSAR 3D (v.12.0.1) desktop modeling platform was then used to perform docking of ATP (PubChem ID: 5957) to the AC center of the AtAC model via FlexX docking functionality [37] [38]. A structural alignment was conducted by fragment assembly simulations based on iterative templates using the iterative threading assembly refinement (I-TASSER) server to match AtAC to an experimentally-confirmed structure in the PDB library [39]. The model with the highest C-score was analyzed using PyMOL (v.1.7.4.) (Schrödinger LLC, New York, USA) and then adopted in the study.

2.5. Complementation Testing of AtAC$^{260\text{-}388}$

The *E. coli cya*A mutant SP850 strain (lam-, el4-, relA1, spoT1, *cya*A1400 (:kan), thi-1) [40], deficient in the adenylate cyclase (*cya*A) gene, was obtained from the *E. coli* Genetic Stock Centre (Yale University, New Haven, USA) (accession No. 7200). The strain was prepared to be chemically competent followed by its transformation with the pTrcHis2-TOPO:AtAC$^{260\text{-}388}$ fusion construct (through heat shock at 42˚C for 2 min). The transformed bacteria were then grown at 37˚C in Luria-Bertani (LB) media containing ampicillin (100 µg/ml) and kanamycin (15 µg/ml) until their cell density had reached an optical density (OD_{600}) of 0.5. The cells were treated with 0.5 mM isopropyl-β-D-thiogalactopyranoside (IPTG, Sigma-Aldrich Corp., Missouri, USA) for transgene induction, and further incubated for 4 h prior to streaking on MacConkey agar. The streaked plate was then incubated for 40 h at 37˚C before being visually inspected. After incubation, an ability of the induced transformed mutant cells to now ferment lactose would then be considered as an indication of the expressed recombinant AtAC$^{260\text{-}388}$'s ability to generate cAMP from ATP, as a functional AC. As a result, the induced transformed cells would then turn deep red or purple while control cells (mutant or cells not expressing the AtAC$^{260\text{-}388}$) would remain yellow or colorless [15] [21] [24].

2.6. Statistical Analysis

Data, in triplicate sets (n = 3), was subjected to analysis of variance (ANOVA) (Super-Anova, Statsgraphics Version 7, Statsgraphics Corp., The Plains, VI, USA). Where ANOVA revealed significant differences between treatments, means were separated by the *post hoc* Student-Newman-Keuls (SNK) multiple range test ($p < 0.05$).

3. Results

3.1. Determination of the *in Vitro* AC Activity of AtAC$^{260\text{-}388}$

In higher plants, the identification of ACs mostly involved querying protein se-

quences with an AC motif (**Figure 1(a)**) derived from a guanylyl cyclase (GC) search motif [41] through modification at position 3, changing [CTGH] to [DE] [42]. This modification was primarily based on previous findings, which indicated that the conversion of GCs into ACs and vice versa could be easily achieved through a single mutation in the amino acid that confers substrate specificity [43] [44]. When the amino acid sequence of AtAC was queried by the AC motif, a matching hit was detected towards its C-terminal end (amino acids 336 - 350) (**Figure 1(b)**). A fragment sequence of the At3g21465 gene (amino acids 261 - 388) harboring the AC motif (**Figure 1(b)**) was then cloned into a prokaryotic system and expressed into a 17.580 kDa $AtAC^{261\text{-}388}$ His-tagged recombinant protein (**Figure 1(c)**).

To check if the AC center of AtAC can generate cAMP *in vitro*, the expressed recombinant $AtAC^{261\text{-}388}$ was extracted and affinity purified (**Figure 1(d)**, inset). The AC activity of the purified recombinant was then tested in a reaction mixture containing ATP as substrate, Mn^{2+} or Mg^{2+} as cofactor, and Ca^{2+} or HCO_3^- as modulator, followed by measurement of cAMP by enzyme immunoassay. Maximum activity was reached after 20 minutes of the reaction system, generating about 86 fmols/μg protein of cAMP in the presence of Mn^{2+} and approximately 25 fmols/μg protein of cAMP in the presence of Mg^{2+} compared to only about 13 fmols/μg protein of cAMP of the control reaction (**Figure 1(d)**). Besides being Mn^{2+}-dependent, the catalytic activity of $AtAC^{261\text{-}388}$ was also significantly enhanced by both Ca^{2+} and HCO_3^-, reaching activity levels of around 141 and 124 fmols/μg protein of cAMP respectively when Mn^{2+} is the co-factor (**Figure 1(d)**).

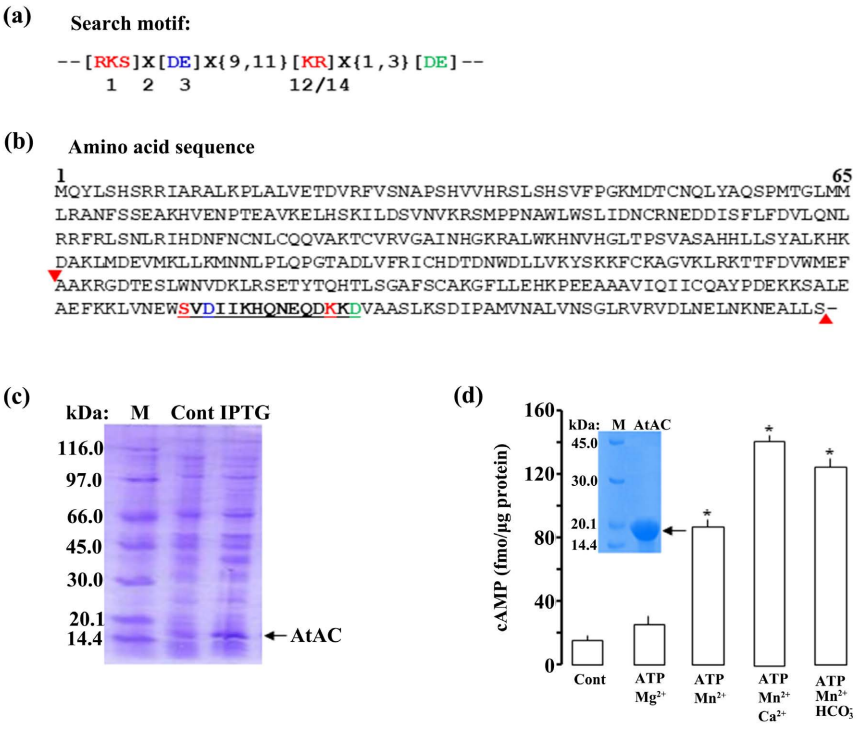

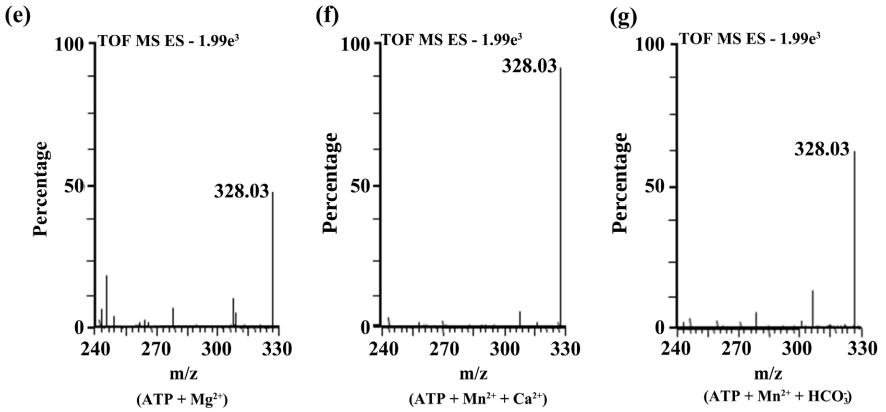

Figure 1. (a) The 14 amino acid AC search motif derived from annotated and experimentally tested GC and AC catalytic centres. The residue forming hydrogen bonding with purine at position 1 is highlighted in red, the residue conferring substrate specificity in position 3 is highlighted in blue, while the amino acid in position 14, stabilizing the transition state from ATP to cAMP, is highlighted in red. The amino acid [DE] at 1 - 3 residues downstream from position 14, participates in Mg^{2+}/Mn^{2+}-binding and is coloured green. (b) The complete amino acid sequence of AtAC with the AC catalytic center towards its C-terminus (amino acids 336 - 350) highlighted in bold and underline, and the 128 amino acid sequence fragment tested for AC activity indicated within the inverted red triangles. (c) Sodium dodecyl sulfate–polyacrylamide gel electrophoresis (SDS-PAGE) of protein fractions (stained with Coomassie brilliant blue) from the induced (IPTG) and un-induced (Cont) cell cultures, where (M) is the molecular weight marker and the arrow marking the expressed recombinant $AtAC^{261-388}$ protein. (d) cAMP generated by 5 µg recombinant $AtAC^{261-388}$ in the presence of 1 mM ATP and 5 mM Mn^{2+} or Mg^{2+}, or 1 mM ATP and 250 µM Ca^{2+} or 50 mM HCO_3^- when 5 mM Mn^{2+} ion is the cofactor. Control reaction contained all other components except the protein, Ca^{2+} and HCO_3^-. Inset: A Coomassie brilliant blue-stained gel after resolution of the affinity purified His-tagged recombinant $AtAC^{261-388}$ (arrow) by SDS-PAGE. Extracted mass chromatograms of the m/z 328 $[M-1]^{-1}$ ion of cAMP generated by 5 µg recombinant $AtAC^{261-388}$ in a reaction mixture containing (e) 1 mM ATP and 5 mM Mn^{2+} or (f) 1 mM ATP, 5 mM Mn^{2+} and 250 µM Ca^{2+} or (g) 1 mM ATP, 5 mM Mn^{2+} and 50 mM HCO_3^-. Data are mean values (n = 3) and error bars show standard error (SE) of the mean. Asterisks denote values significantly different from those of control ($p < 0.05$) determined by analysis of variance (ANOVA) and *post hoc* Student-Newman-Keuls (SNK) multiple range tests.

cAMP was also measured by mass spectrometry. In a reaction mixture containing $AtAC^{261-388}$ alone, 48.0% cAMP was detected (**Figure 1(e)**), whereas in a reaction mixture supplemented with Ca^{2+}, 90.5% cAMP was detected (**Figure 1(f)**) and in a reaction mixture supplemented with HCO_3^-, 62.3% was detected (**Figure 1(g)**). This additional method therefore, confirmed presence of cAMP in the reaction mixtures, thereby validating the enzyme immunoassay technique and confirming function for the AC center of AtAC.

3.2. Computational Assessment and Complementation Testing of AtAC

In addition to the determination of activity of the AC center of AtAC using enzyme immunoassay and mass spectrometry, we also used computational me-

thods to assess the feasibility of this center to bind the substrate (ATP) and catalyze its subsequent conversion into cAMP. We prepared the full-length AtAC model by artificial intelligence and showed that in this model, the AC center is solvent-exposed, thus allowing for unimpeded substrate interactions and presumably catalysis (Figures 2(a)-(d)). To test if the AC center can rescue an *E. coli*

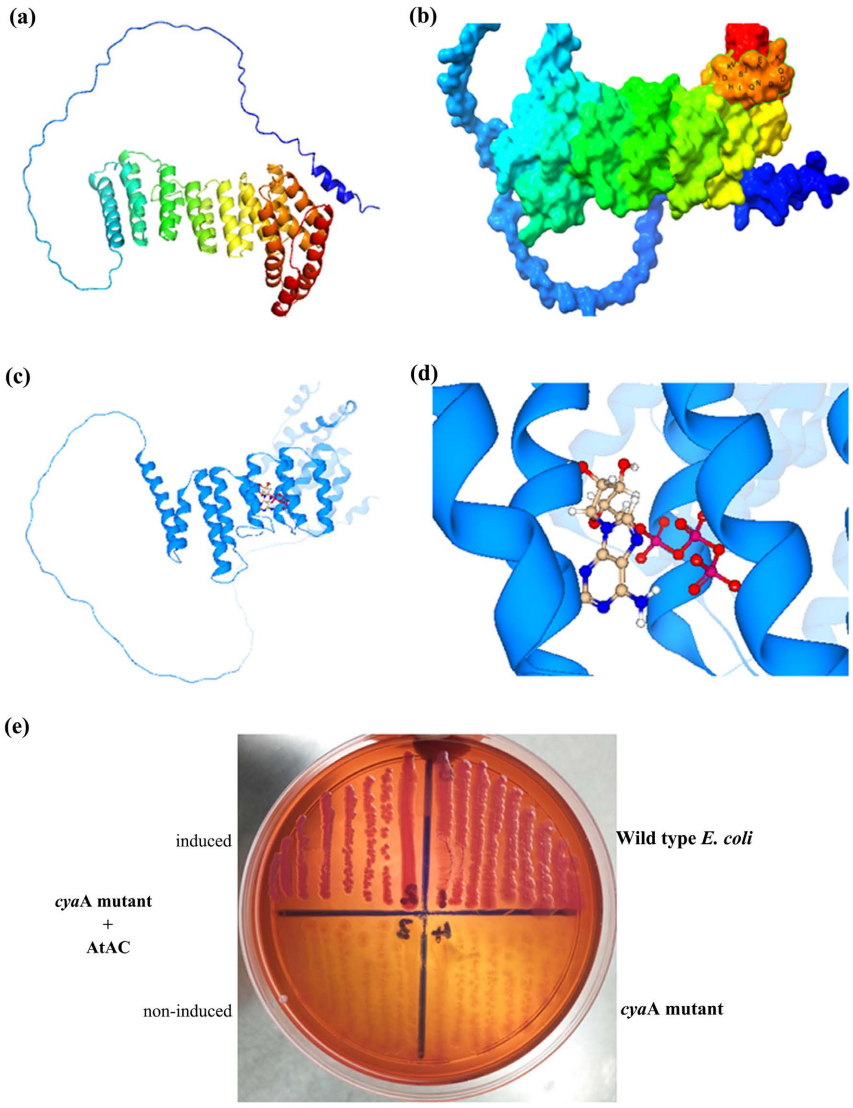

Figure 2. Full-length models of AtAC showing the AC center (gold) in the AlphaFOLD-derived (a) ribbon model (N → C: blue → red) and (b) surface model (highlighting the solvent-exposed AC center). Residues of the AC center are labelled with single letter codes in black. Docking of ATP at the AC center and interaction of ATP with key residues at the catalytic center of AtAC shown as (c) ball (purine head) and stick (phosphate tail) and (d) adenosine (blue) and phosphate (red) groups straddling the parallel beta helices in the surface model. AtAC was modelled using AlphaFOLD [35] and ATP docking simulation was performed using the FlexX functionality of SeeSAR (v12.0.1) [37]. (e) The AC center complemented a *cya*A mutant *E. coli* (SP850) to ferment lactose. Wild-type and $AtAC^{261-388}$-expressing SP850 *E. coli* cells showed a strong reddish color while both the *cya*A mutant and *cya*A mutant cells with an un-induced recombinant $AtAC^{261-388}$ yielded yellowish colonies.

AC-deficient mutant, the AtAC$^{261\text{-}388}$ recombinant was expressed in an *E. coli* SP850 strain lacking the AC (*cya*A), essential for lactose fermentation [40] [45] [46]. As a result of the *cya*A mutation, the AC deficient and un-induced transformed *E. coli* cells remained yellowish in color when grown on MacConkey agar. In contrast, the AtAC$^{261\text{-}388}$-expressing SP850 cells formed deep reddish colonies much like the wild-type *E. coli* (**Figure 2(e)**) thus indicating a functional AC center in the recombinant AtAC$^{261\text{-}388}$ protein.

4. Discussion

In *Arabidopsis thaliana* and *Zea mays*, the discovery of candidate ACs has been through a systematic approach, which involved identification of key amino acid residues in the catalytic center of known and experimentally tested nucleotide cyclases (NCs) [41] [42]. In that approach, a GC search motif [41] at position 3, was changed from [CTGH] to [DE] to generate a rationally designed search motif specific for ACs (**Figure 1(a)**) [42]. This substitution was based on previous findings, which indicated that the conversion of GCs into ACs and *vice versa* could be achieved by a single mutation in the amino acid residue that confers substrate specificity [43] [44]. Using this systematic approach, a total of six candidate ACs have so far been discovered in Arabidopsis, which are AtPPR-AC [24], AtKUP7 [25], AtClAP [26], AtKUP5 [27], AtLRRAC1 [28] [29], and AtNCED3 [30] and one in maize, which is ZmRPP13-LK3 [31]. AtPPR-AC is annotated to play a role in chloroplast biogenesis and restoration of cytoplasmic male sterility [24] while AtClAP is predicted to have a role in endocytosis and plant defense [26]. The two AtKUPs are responsible for K^+ ion flux [25] [27]. AtLRRAC1 has a role in pathogen defense [28] [29] while AtNCED3 is involved in biosynthesis of the stress hormone abscisic acid (ABA) [30]. ZmRPP13-LK3 participates in ABA-mediated resistance to heat stress [31]. Other non-Arabidopsis plant ACs also known to harbour the same rationally designed AC search motif include a *Z. mays* ZmPSiP responsible for the polarized growth of pollen tubes and re-orientation [15], and a *Nicotiana benthamiana* NbAC that plays a role in tabtoxinine-β-lactam-induced cell death during the development of wildfire disease [20].

In *A. thaliana*, besides those six confirmed ACs, there is also another additional putative protein (encoded by the At3g21465 gene) annotated at NCBI (https://www.ncbi.nlm.nih.gov/protein/51968402). This protein harbours the rationally designed AC search motif (**Figure 1(b)**) but however, has no any other annotated domains or known functions and also does not share any similarity with any annotated and/or experimentally confirmed AC but rather appears to be transcriptionally up-regulated in response to biotic stress. Therefore, after functionality of the rationally designed AC search motif was confirmed in *A. thaliana* and other related higher plant species, we then sought to assess and establish if this additional Arabidopsis protein candidate could also be an AC.

We cloned a fragment of the At3g21465 gene and expressed a truncated ver-

sion of the AtAC protein ($AtAC^{261-388}$) harboring the AC search motif (**Figure 1(b)**) as a His-tagged fusion recombinant product of approximately 17.580 kDa (**Figure 1(c)**). When purified (**Figure 1(d)**, inset) and tested for AC activity *in vitro*, using enzyme immunoassay, recombinant $AtAC^{261-388}$ showed a Mn^{2+}-dependent activity that is positively enhanced by calcium and hydrogen carbonate (**Figure 1(d)**). This same result was also obtained via tandem liquid chromatography mass spectrometry (LC-MS/MS) (**Figures 1(e)-(g)**), another method capable of specifically and sensitively detecting cAMP levels at femtomolar concentrations. Thus validating the enzyme immunoassay technique and also confirming the AC function of the $AtAC^{261-388}$ recombinant protein.

Apparently, the ability of $AtAC^{261-388}$ to exhibit a relatively higher (~3.5 fold) AC activity with Mn^{2+} than Mg^{2+} strongly points to AtAC as a soluble AC (sAC) because all sACs prefer Mn^{2+} to Mg^{2+} ion as a co-factor of activity and are intracellularly localized [47]. In *A. thaliana*, AtAC is localized in the mitochondrion (https://www.arabidopsis.org/). Moreover, the activation of $AtAC^{261-388}$ by both Ca^{2+} (~1.6 fold) and HCO_3^- (~1.4 fold) then confirms AtAC as a sAC because only sACs and not transmembrane ACs (tmACs) are functionally activated by these two ions [48] [49]. This kind of activation has previously been observed, wherein activation by Ca^{2+} was thought to be through an invocation of structural changes to the AC center [26] [29] while that by HCO_3^- was through the alteration of pH [49].

Besides our ability to determine the AC activity of AtAC by enzyme immunoassay and mass spectrometry (**Figure 1**), our computational analysis (using artificial intelligence) of the full length AtAC model, showed that its AC center is solvent-exposed, indicating that ATP may have an impeded access to the center and presumably be a substrate for catalysis (**Figures 2(a)-(d)**). To support this, iterative threading assembly refinement (I-TASSER) predicted that AtAC is structurally analogous to pentatricopeptide (PPR) protein [50], a previously confirmed AC [24].

To validate the AC activity of AtAC, we expressed $AtAC^{261-388}$ in a *cya*A *Escherichia coli* mutant strain (SP850) to see if the mutant could be rescued by the $AtAC^{261-388}$. This mutant strain lacks the only AC system available in *E. coli*, necessary for lactose fermentation, therefore, its rescue by any foreign protein to metabolize lactose, signifies AC function for such a protein [40] [45] [46]. In our case, $AtAC^{261-388}$ rescued the SP850 strain (**Figure 2(e)**), consistent with the other ten ACs previously identified in plants [15] [21] [24]-[32].

5. Conclusion

This study provides practical evidence that the putative AtAC protein, which currently has no assigned function in *A. thaliana*, is a *bona fide* AC. This protein thus becomes the seventh and twelfth ever such molecule to be identified in *A. thaliana* and plants, respectively. Considering that this protein has been noted to be transcriptionally up-regulated in response to biotic stress, it is, therefore, cru-

cial that more work is undertaken to try and understand a possible link between this kind of expression and its now determined activity as an AC.

Acknowledgements

This work was funded by North-West University (NWU) and the National Research Foundation (NRF) of South Africa (Grant Numbers: CSUR78843 & CSUR93635).

Author Contribution Statement

OR conceived the idea and designed the study; KSS and TBD did enzyme-immunoassay; EDB and AS did mass spectrometry; DTK did complementation testing; PC designed the models; OR wrote the manuscript; and all authors read, edited, and approved the manuscript.

Conflicts of Interest

The authors declare no conflict of interest.

References

[1] Robison, G.A., Butcher, R.W. and Sutherland, E.W. (1968) Cyclic AMP. *Annual Review of Biochemistry*, **37**, 149-174. https://doi.org/10.1146/annurev.bi.37.070168.001053

[2] Goodman, D.B., Rasmussen, H., Dibella, F. and Guthrow, C.E. (1970) Cyclic Adenosine 3':5'-Monophosphate Stimulated Phosphorylation of Isolated Neuro-Tubule Subunits. *Proceedings of the National Academy of Sciences of the United States of America*, **67**, 652-659. https://doi.org/10.1073/pnas.67.2.652

[3] Gerisch, G., Hulser, D., Malchow, D. and Wick, U. (1975) Cell Communication by Periodic Cyclic-AMP Pulses. *Philosophical Transactions of the Royal Society of London. Series B, Biological Sciences*, **272**, 181-192. https://doi.org/10.1098/rstb.1975.0080

[4] Ashton, A.R. and Polya, G.M. (1978) Cyclic Adenosine 3',5'-Monophosphate in Axenic Rye Grass Endosperm Cell Cultures. *Plant Physiology*, **61**, 718-722. https://doi.org/10.1104/pp.61.5.718

[5] Buck, J., Sinclair, M.L., Schapal, L., Cann, M.J. and Levin, L.R. (1999) Cytosolic Adenylyl Cyclase Defines a Unique Signaling Molecule in Mammals. *Proceedings of the National Academy of Sciences of the United States of America*, **96**, 79-84. https://doi.org/10.1073/pnas.96.1.79

[6] Amrhein, N. (1977) The Current Status of Cyclic AMP in Higher Plants. *Annual Review of Plant Physiology*, **28**, 123-132. https://doi.org/10.1146/annurev.pp.28.060177.001011

[7] Meier, S., Ruzvidzo, O., Morse, M., Donaldson, L., Kwezi, L. and Gehring, C. (2010) The Arabidopsis Wall Associated Kinase-Like 10 Gene Encodes a Functional Guanylyl Cyclase and Is Co-Expressed with Pathogen Defense Related Genes. *PLOS ONE*, **5**, e8904. https://doi.org/10.1371/journal.pone.0008904

[8] Kurosaki, F., Kaburaki, H. and Nishi, A. (1993) Synthesis and Degradation of Cyclic AMP in Cultured Carrot Cells Treated with Forskolin. *Archives of Biochemistry and Biophysics*, **303**, 177-179. https://doi.org/10.1006/abbi.1993.1270

[9] Carricarte, V.C., Bianchini, G.M., Muschietti, J.P., Tellez-Inon, M.T., Perticari, A., Torres, N. and Flawia, M.M. (1988) Adenylate Cyclase Activity in a Higher Plant, Alfalfa (*Medicago sativa*). *The Biochemical Journal*, **249**, 807-811. https://doi.org/10.1042/bj2490807

[10] Li, W., Luan, S., Schreiber, S.L. and Assmann, S.M. (1994) Cyclic AMP Stimulates K^+ Channel Activity in Mesophyll Cells of *Vicia faba* L. *Plant Physiology*, **106**, 957-961. https://doi.org/10.1104/pp.106.3.957

[11] Ehsan, H., Reichheld, J.P., Roef, L., Witters, E., Lardon, F., Van Bockstaele, D., Van Montagu, M., Inzé, D. and Van Onckelen, H. (1998) Effect of Indomethacin on Cell Cycle Dependent Cyclic AMP Fluxes in Tobacco BY-2 Cells. *FEBS Letters*, **422**, 165-169. https://doi.org/10.1016/S0014-5793(97)01610-4

[12] Maathuis, F.J. and Sanders, D. (2001) Sodium Uptake in Arabidopsis Roots Is Regulated by Cyclic Nucleotides. *Plant Physiology*, **127**, 1617-1625. https://doi.org/10.1104/pp.010502

[13] Jin, X.C. and Wu, W.H. (1999) Involvement of Cyclic AMP in ABA- and Ca^{2+}-Mediated Signal Transduction of Stomatal Regulation in *Vicia faba*. *Plant Cell Physiology* **40**, 1127-1133. https://doi.org/10.1093/oxfordjournals.pcp.a029497

[14] Tezuka, T., Hiratsuka, S. and Takahashi, S.Y. (1993) Promotion of the Growth of Self-Incompatible Pollen Tubes in Lily by cAMP. *Plant and Cell Physiology*, **34**, 955-958.

[15] Moutinho, A., Hussey, P.J., Trewavas, A.J. and Malhó, R. (2001) cAMP Acts as a Second Messenger in Pollen Tube Growth and Re-Orientation. *Proceedings of the National Academy of Sciences of the United States of America*, **98**, 10481-10486. https://doi.org/10.1073/pnas.171104598

[16] Bolwell, G.P. (1992) A Role for Phosphorylation in the Down-Regulation of Phenylalanine Ammonia-Lyase in Suspension-Cultured Cells of French Bean. *Phytochemistry*, **31**, 4081-4086. https://doi.org/10.1016/0031-9422(92)80418-E

[17] Pietrowska-Borek, M. and Nuc, K. (2013) Both Cyclic-AMP and Cyclic-GMP Can Act as Regulators of the Phenylpropanoid Pathway in *Arabidopsis thaliana* Seedlings. *Plant Physiology and Biochemistry*, **70**, 142-149. https://doi.org/10.1016/j.plaphy.2013.05.029

[18] Choi, Y.E. and Xu, J.R. (2010) The cAMP Signaling Pathway in *Fusarium verticillioides* Is Important for Conidiation, Plant Infection, and Stress Responses But Not Fumonisin Production. *Molecular Plant-Microbe Interactions*, **23**, 522-533. https://doi.org/10.1094/MPMI-23-4-0522

[19] Thomas, L., Marondedze, C., Ederli, L., Pasqualini, S. and Gehring, C. (2013) Proteomic Signatures Implicate cAMP in Light and Temperature Responses in *Arabidopsis thaliana*. *Journal of Proteomics*, **83**, 47-59. https://doi.org/10.1016/j.jprot.2013.02.032

[20] Ito, M., Takahashi, H., Sawasaki, T., Ohnishi, K., Hikichi, Y. and Kiba, A. (2014) Novel Type of Adenylyl Cyclase Participates in Tabtoxinine-β-lactam-Induced Cell Death and Occurrence of Wildfire Disease in *Nicotiana benthamiana*. *Plant Signaling and Behavior*, **9**, e27420. https://doi.org/10.4161/psb.27420

[21] Swieżawska, B., Jaworski, K., Pawełek, A., Grzegorzewska, W., Szewczuk, P. and Szmidt-Jaworska, A. (2014) Molecular Cloning and Characterization of a Novel Adenylyl Cyclase Gene, HpAC1, Involved in Stress Signaling in *Hippeastrum hybridum*. *Plant Physiology and Biochemistry*, **80**, 41-52. https://doi.org/10.1016/j.plaphy.2014.03.010

[22] Zelman, A.K., Dawe, A., Gehring, C. and Berkowitz, G.A. (2012) Evolutionary and

Structural Perspectives of Plant Cyclic Nucleotide-Gated Cation Channels. *Frontiers in Plant Science*, **3**, Article No. 95. https://doi.org/10.3389/fpls.2012.00095

[23] Gehring, C. and Turek, I.S. (2017) Cyclic Nucleotide Monophosphates and Their Cyclases in Plant Signaling. *Frontiers in Plant Science*, **8**, Article No. 1704. https://doi.org/10.3389/fpls.2017.01704

[24] Ruzvidzo, O., Dikobe, B.T., Kawadza, D.T., Mabadahanye, G.H., Chatukuta, P. and Kwezi, L. (2013) Recombinant Expression and Functional Testing of Candidate Adenylate Cyclase Domains. *Methods in Molecular Biology*, **1016**, 13-25. https://doi.org/10.1007/978-1-62703-441-8_2

[25] Al-Younis, I., Wong, A. and Gehring, C. (2015) The *Arabidopsis thaliana* K^+-Uptake Permease 7 (AtKUP7) Contains a Functional Cytosolic Adenylate Cyclase Catalytic Centre. *FEBS Letters*, **589**, 3848-3852. https://doi.org/10.1016/j.febslet.2015.11.038

[26] Chatukuta, P., Dikobe, T.B., Kawadza, D.T., Sehlabane, K.S., Takundwa, M.M., Wong, A., Gehring, C. and Ruzvidzo, O. (2018) An Arabidopsis Clathrin Assembly Protein with a Predicted Role in Plant Defense Can Function as an Adenylate Cyclase. *Biomolecules*, **8**, Article 15. https://doi.org/10.3390/biom8020015

[27] Al-Younis, I., Wong, A., Lemtiri-Chlieh, F., Schmöckel, S., Tester, M., Gehring, G. and Donaldson, L. (2018) The *Arabidopsis thaliana* K^+-Uptake Permease 5 (AtKUP5) Contains a Functional Cytosolic Adenylate Cyclase Essential for K^+ Transport. *Frontiers in Plant Science*, **9**, Article No. 1645. https://doi.org/10.3389/fpls.2018.01645

[28] Bianchet, C., Wong, A., Quaglia, M., Alqurashi, M., Gehring, C., Ntoukakis, V. and Pasqualini, S. (2019) An *Arabidopsis thaliana* Leucine-Rich Repeat Protein Harbors an Adenylyl Cyclase Catalytic Center and Affects Responses to Pathogens. *Journal of Plant Physiology*, **232**, 12-22. https://doi.org/10.1016/j.jplph.2018.10.025

[29] Ruzvidzo, O., Gehring, C. and Wong, A. (2019) New Perspectives on Plant Adenylyl Cyclases. *Frontiers in Molecular Biosciences*, **6**, Article No. 136. https://doi.org/10.3389/fmolb.2019.00136

[30] Al-Younis, I., Moosa, B., Kwiatkowski, M., Jaworski, K., Wong, A. and Gehring, C. (2021) Functional Crypto-Adenylate Cyclases Operate in Complex Plant Proteins. *Frontiers in Plant Science*, **12**, Article No. 1709. https://doi.org/10.3389/fpls.2021.711749

[31] Yang, H., Zhao, Y., Chen, N., Liu, Y., Yang, S., Du, H., Wang, W., Wu, J., Tai, F., Chen, F. and Hu, X. (2021) A New Adenylyl Cyclase, Putative Disease-Resistance RPP13-Like Protein 3, Participates in Abscisic Acid-Mediated Resistance to Heat Stress in Maize. *Journal of Experimental Botany*, **72**, 283-301. https://doi.org/10.1093/jxb/eraa431

[32] Kasahara, M., Suetsugu, N., Urano, Y., Yamamoto, C., Ohmori, M., Takada, Y., Okuda, S., Nishiyama, T., Sakayama, H., Kohchi, T. and Takahashi, F. (2016) An Adenylyl Cyclase with a Phosphodiesterase Domain in Basal Plants with a Motile Sperm System. *Scientific Reports*, **6**, Article No. 39232. https://doi.org/10.1038/srep39232

[33] Kwezi, L., Ruzvidzo, O., Wheeler, J.I., Govender, K., Iacuone, S., Thompson, P.E., Gehring, C. and Irving, H.R. (2011) The Phytosulfokine (PSK) Receptor Is Capable of Guanylate Cyclase Activity and Enabling Cyclic GMP-Dependent Signaling in Plants. *Journal of Biological Chemistry*, **286**, 22580-22588. https://doi.org/10.1074/jbc.M110.168823

[34] Bradford, M.A. (1976) Rapid and Sensitive Method for the Quantitation of Micro-

gram Quantities of Protein Utilizing the Principle of Protein-Dye Binding. *Analytical Biochemistry*, ***72***, 248-254. https://doi.org/10.1016/0003-2697(76)90527-3

[35] Varadi, M., Anyango, S., Deshpande, M., Nair, S., Natassia, C., Yordanova, G., Yuan, D., Stroe, O., Wood, G., Laydon, A., Žídek, A., Green, T., Tunyasuvunakool, K., Petersen, S., Jumper, J., Clancy, E., Green, R., Vora, A., Lutfi, M., Figurnov, M. and Velankar, S. (2022) AlphaFold Protein Structure Database: Massively Expanding the Structural Coverage of Protein-Sequence Space with High-Accuracy Models. *Nucleic Acids Research*, **50**, D439-D444. https://doi.org/10.1093/nar/gkab1061

[36] Pettersen, E.F., Goddard, T.D., Huang, C.C., Meng, E.C., Couch, G.S., Croll, T.I., Morris, J.H. and Ferrin, T.E. (2021) UCSF ChimeraX: Structure Visualization for Researchers, Educators, and Developers. *Protein Science*, **30**, 70-82. https://doi.org/10.1002/pro.3943

[37] Gastreich, M., Lilienthal, M., Briem, H. and Claussen, H. (2006) Ultrafast *De Novo* Docking Combining Pharmacophores and Combinatorics. *Journal of Computer-aided Molecular Design*, **20**, 717-734. https://doi.org/10.1007/s10822-006-9091-x

[38] Trott, O. and Olson, A.J. (2010) Software News and Update AutoDock Vina: Improving the Speed and Accuracy of Docking with a New Scoring Function, Efficient Optimization, and Multithreading. *Journal of Computional Chemistry*, **31**, 455-461. https://doi.org/10.1002/jcc.21334

[39] Zhang, Y. (2008) I-TASSER Server for Protein 3D Structure Prediction. *BMC Bioinformatics*, **9**, Article No. 40. https://doi.org/10.1186/1471-2105-9-40

[40] Shah, S. and Peterkofsky, A. (1991) Characterization and Generation of *Escherichia coli* Adenylate Cyclase Deletion Mutants. *Journal of Bacteriology*, **173**, 3238-3242. https://doi.org/10.1128/jb.173.10.3238-3242.1991

[41] Ludidi, N. and Gehring, C. (2003) Identification of a Novel Protein with Guanylyl Cyclase Activity in *Arabidopsis thaliana*. *Journal of Biological Chemistry*, **278**, 6490-6494. https://doi.org/10.1074/jbc.M210983200

[42] Gehring, C. (2010) Adenyl Cyclases and cAMP in Plant Signaling—Past and Present. *Cell Communication and Signalling*, **8**, Article No. 15. https://doi.org/10.1186/1478-811X-8-15

[43] Tucker, C.L., Hurley, J.H., Miller, T.R. and Hurley, J.B. (1998) Two Amino Acid Substitutions Convert a Guanylyl Cyclase, RetGC-1, into an Adenylyl Cyclase. *Proceedings of the National Academy of Sciences of the United States of America*, **95**, 5993-5997. https://doi.org/10.1073/pnas.95.11.5993

[44] Roelofs, J., Meima, M., Schaap, P. and Van Haastert, P.J. (2001) The Dictyostelium Homologue of Mammalian Soluble Adenylyl Cyclase Encodes a Guanylyl Cyclase. *EMBO Journal*, **20**, 4341-4348. https://doi.org/10.1093/emboj/20.16.4341

[45] Ullmann, A. and Danchin, A. (1980) Role of Cyclic AMP in Regulatory Mechanisms in Bacteria. *Trends Biochemical Sciences*, **5**, 95-96. https://doi.org/10.1016/0968-0004(80)90257-1

[46] Tang, W.J. and Gilman, A.G. (1995) Construction of a Soluble Adenylyl Cyclase Activated by Gs Alpha and Forskolin. *Science*, **268**, 1769-1772. https://doi.org/10.1126/science.7792604

[47] Braun, T. and Dods, R.F. (1975) Development of a Mn^{2+}-Sensitive, "Soluble" Adenylate Cyclase in Rat Testis. *Proceedings of the National Academy of Sciences of the United States of America*, **72**, 1097-1101. https://doi.org/10.1073/pnas.72.3.1097

[48] Steer, M.L. and Levitzki, A. (1975) The Interaction of Catecholamines, Ca^{2+} and Adenylate Cyclase in the Intact Turkey Erythrocyte. *Archives of Biochemistry and Biophysics*, **167**, 371-376. https://doi.org/10.1016/0003-9861(75)90473-7

[49] Chen, Y., Cann, M.J., Litvin, T.N., Iourgenko, V., Sinclair, M.L., Levin, L.R. and Buck, J. (2000) Soluble Adenylyl Cyclase as an Evolutionarily Conserved Bicarbonate Sensor. *Science*, **289**, 625-628. https://doi.org/10.1126/science.289.5479.625

[50] Shen, C., Zhang, D., Guan, Z., Liu, Y., Yang, Z., Yang, Y., Wang, X., Wang, Q., Zhang, Q., Fan, S., Zou, T. and Yin, P. (2016) Structural Basis for Specific Single-stranded RNA Recognition by Designer Pentatricopeptide Repeat Proteins. *Nature Communications*, **7**, Article No. 11285. https://doi.org/10.1038/ncomms11285

Appendix

	Name	Src	Estimated affinity pM	nM	µM	mM	LLE	LE	Tor.	Intra clash
1	5957_2_001									
2	5957_2_002									
3	5957_2_003									
4	5957_2_004									
5	5957_2_005									
6	5957_2_006									
7	5957_2_007									
8	5957_2_008									
9	5957_2_009									
10	59...10									

	MW	LogP	TPSA	2C9 pKi optibrium	2D6 affin... optibrium	BBB categ... optibrium	BBB log([... optibrium	HIA categ... optibrium	P-gp cate... optibrium
1	503.15	-4.16	290.4	4.972	low	-	-1.629	-	yes
2	503.15	-4.16	290.4	4.972	low	-	-1.629	-	yes
3	503.15	-4.16	290.4	4.972	low	-	-1.629	-	yes
4	503.15	-4.16	290.4	4.972	low	-	-1.629	-	yes
5	503.15	-4.16	290.4	4.972	low	-	-1.629	-	yes
6	504.16	-4.74	291.7	4.972	low	-	-1.629	-	yes
7	504.16	-4.74	291.7	4.972	low	-	-1.629	-	yes
8	503.15	-4.16	290.4	4.972	low	-	-1.629	-	yes
9	503.15	-4.16	290.4	4.972	low	-	-1.629	-	yes
10	503.15	-4.16	290.4	4.972	low	-	-1.629	-	yes

	PPB90 cat... optibrium	hERG pIC5... optibrium	logD optibrium	logP optibrium	logS optibrium	logS @ pH... optibrium	SDF13	SDF14	SDF15
1	low	2.744	-1.204	-0.163	3.264	4.005	4	0	0
2	low	2.744	-1.204	-0.163	3.264	4.005	4	0	0
3	low	2.744	-1.204	-0.163	3.264	4.005	4	0	0
4	low	2.744	-1.204	-0.163	3.264	4.005	4	0	0
5	low	2.744	-1.204	-0.163	3.264	4.005	4	0	0
6	low	2.744	-1.204	-0.163	3.264	4.005	4	0	0
7	low	2.744	-1.204	-0.163	3.264	4.005	4	0	0
8	low	2.744	-1.204	-0.163	3.264	4.005	4	0	0
9	low	2.744	-1.204	-0.163	3.264	4.005	4	0	0
10	low	2.744	-1.204	-0.163	3.264	4.005	4	0	0